

Model-free fast charging of lithium-ion batteries by online gradient descent

Hamed Taghavian, Malin Andersson, and Mikael Johansson

Abstract—A data-driven solution is provided for the fast-charging problem of lithium-ion batteries with multiple safety and aging constraints. The proposed method optimizes the charging current based on the observed history of measurable battery quantities, such as the input current, terminal voltage, and temperature. The proposed method does not need any detailed battery model or full-charging training episodes. The theoretical convergence is proven under mild conditions and is validated numerically on several linear and nonlinear battery models, including single-particle and equivalent-circuit models.

I. INTRODUCTION

Whether it be trains, road vehicles, or boats, electrified transportation is believed to have a positive impact on both the ecology and the economy. Among the different energy storage units available for electrified transportation, lithium-ion batteries are expected to remain the dominant option for at least a decade, due to their many favorable properties [17].

Despite their numerous advantages, however, electric vehicles equipped with lithium-ion batteries suffer from long charging times compared to conventional gasoline-fueled vehicles [11]. Simply increasing the charging current does not solve this problem due to the safety and degradation issues associated with high charging currents. Hence, a recent line of research has focused on developing charging protocols that maximize the charging current while accounting for battery health and safety [21].

Obtaining such optimal charging protocols normally requires accurate models of the battery dynamics which are not always available. Identifying the parameters that determine the dynamic behavior of lithium-ion batteries is difficult [9] and there are several factors, such as aging, ambient conditions, etc., that can cause the actual dynamics to drift away from those of a previously identified model. Therefore, several model-free charging techniques have been proposed that avoid system identification and instead operate directly based on observing the data collected from the lithium-ion batteries in real-world operation. Available approaches include Bayesian optimization [8], iterative learning control [22] and reinforcement learning [3]. To converge to the optimal charging protocol, these methods rely on a learning process over several full-charging episodes. Such charging experiments are time-consuming and degrade the batteries.

In this paper, we first note that the optimal solutions to typical fast-charging problems are of the bang-ride form, that

is, they operate on the boundary of the feasible set [2]. This property has already been proven for various fast-charging problems [20, 1, 14] and conjectured to be true for several others [10]. The industry standard for fast charging of lithium-ion batteries, the Constant-Current-Constant-Voltage (CCCV) charging protocol, is of bang-ride form, with an initial phase where the maximal current is applied (bang), followed by a phase where the current is gradually decreased to maintain a constant terminal voltage (ride). We exploit this fact to design a data-driven controller with a fixed structure that converges to the bang-ride charging protocols in real-time, without requiring any prior training episodes. The proposed approach is less costly than other model-free methods, as it does not need additional charging experiments.

The proposed controller uses measured input-output data of the battery to learn its bang-ride protocol, without relying on a battery model or access to the cost function in the fast-charging problem. The protocol does not need to know the functional form of the constraints, it only assumes that constraint violations can be measured. Our proposed control structure has a similar switching nature to [10]. However, the approach in [10] requires a full model and its parameters and does not provide a technique for tuning the PI controllers nor proves convergence to the desired charging protocol. In contrast, we propose an adaptive feedback controller that guarantees convergence to the bang-ride protocol without a battery model or manual tuning of the controllers.

Convergence to the bang-ride protocol is realized by solving an online convex optimization problem. Online convex optimization is an adaptation of convex optimization algorithms to unknown and changing environments [24]. In these problems, the cost function changes in every time step, and the algorithm only has access to the previous set of cost functions and decision variables [4]. An additional complexity emerges when the cost functions in different time steps are coupled [12, 18]. This happens in optimal control problems [12] as well as in fast-charging problems since there is an underlying dynamic system that affects the cost functions in the overall optimization process. Nevertheless, the online optimization-based algorithm proposed in this paper can achieve a sublinear regret similar to the uncoupled case [24], and contrary to [12], it does not require linearity of the dynamics and strong convexity of the cost functions. Furthermore, in contrast with other learning-based control systems [6], such as iterative feedback tuning (IFT) [5] and simultaneous perturbation stochastic approximation (SPSA) [19], the monotone properties specific to fast charging problems are exploited to avoid estimating the gradient directions.

This work was supported by KTH Royal Institute of Technology. The authors are with the Division of Decision and Control Systems, KTH Royal Institute of Technology. Emails: hamedta@kth.se, malinan9@kth.se, mikaelj@kth.se.

Thus, the charging current is not disrupted by running experiments during the learning process.

This paper is structured as follows. We define the fast-charging optimization problems in Section II, develop a model-free fast-charging algorithm based on online gradient descent in Section III, and present a few case studies for numerical evaluation in Section IV. Conclusive remarks and potential future research directions are provided in Section V.

II. FAST CHARGING AND BANG-RIDE PROTOCOLS

Consider a discrete-time battery model of the form

$$x_{t+1} = f(x_t, u_t), \quad t \in \mathbb{N}_0 \quad (1a)$$

$$y_{i,t} = h_i(x_t, u_t), \quad i = 1, 2, \dots, p \quad (1b)$$

where $x_t \in \mathbb{R}^n$ is the battery state, $y_{i,t} \in \mathbb{R}$ are the measurable outputs and $u_t \in \mathbb{R}$ is the input current. As a convention, u_t is positive when we charge (feed current into the battery). A general fast-charging optimization problem with multiple constraints can be stated as

$$\begin{aligned} & \underset{u}{\text{maximize}} && J(x_0, u) = \sum_{t=0}^{t_f} L(x_t, u_t) \\ & \text{subject to} && y_{i,t} \leq \bar{y}_i, \quad i = 1, 2, \dots, p \\ & && x, u, y_i \text{ satisfy (1)} \end{aligned} \quad (2)$$

where $x_0 \in \mathbb{R}^n$ is the initial state of the battery. We make the following assumption throughout the paper.

Assumption 1: The output functions $h_i(x_t, u_t)$ are differentiable and strictly increasing in $u_t \in \mathbb{R}$ for all $x_t \in \mathbb{R}^n$.

We assume the first constraint in (2) imposes an explicit upper bound on the charging current, *i.e.*,

$$y_{1,t} = h_1(x_t, u_t) = u_t \leq u_{\max} = \bar{y}_1 \quad (3)$$

In typical fast-charging problems, the running-cost $L(x_t, u_t)$ and transition functions $f(x_t, u_t)$ are continuous and increasing in x_t, u_t , and the constraint functions $h_i(x_t, u_t)$ are continuous and increasing in u_t [2]. This makes (2) a monotone optimal control problem, whose solution is known to touch the feasible set boundaries, regardless of the exact transition, cost, or constraint functions [20]. If the optimal solution operates on the feasible set boundary at all times, *i.e.*, at least one inequality constraint in (2) is active at every time step, then the optimal solution is said to be of bang-ride form. This has shown to be the case for several specific fast-charging problems on the form (2) [1, 14]. More general sufficient conditions that ensure the optimal solution of (2) is of bang-ride form are provided in [20]. Hence in this paper, we provide an algorithm that implements the bang-ride solution of the fast-charging problem (2) when the battery model, the constraints, and the cost function are unknown.

To calculate the bang-ride solution of (2), we note that since the output functions are strictly increasing (Assumption 1), each equation

$$h_i(x_t, u_t) = \bar{y}_i, \quad i = 1, 2, \dots, p \quad (4)$$

has at most one solution, $u_t = K_i(x_t)$ where $K_i: \mathbb{R}^n \rightarrow \mathbb{R}$ is a possibly nonlinear function. For example, for the first

constraint (3), equation (4) has the unique solution

$$u_t = K_1(x_t) = u_{\max}$$

By defining $K_i(x_t) = +\infty$ in case equation (4) has no real solution for u_t , it is possible to write the ideal bang-ride protocol as the following nonlinear state-feedback law

$$u_t = \min\{K_1(x_t), K_2(x_t), \dots, K_p(x_t)\} \quad (5)$$

This expression is well-defined since at least one argument, *i.e.* $K_1(x_t)$, is always finite.

If an accurate model is available and all system states can be measured, the bang-ride control (5) is simple to implement. Even if the feedback functions K_i cannot be determined explicitly, the monotonicity of the output functions makes it easy to solve the constraint equations (4) numerically for a given x_t to determine each $K_i(x_t)$.

In practice, however, battery models are not perfect and the full system state is not measured. It is then considered to be difficult to obtain a high-quality estimate of the model parameters and the state vector x_t [9]. To overcome these challenges, we develop a data-driven implementation of (5) in the next section that does not rely on the system model, does not require the state vector x_t , and does not require solving the constraint equations (4) in every sample.

III. MODEL-FREE CHARGING

A. Active constraint switching

The bang-ride control law (5) effectively determines both which constraint should be active and the control input that keeps the corresponding output at its maximally allowed value. When we do not have access to an accurate model and cannot measure the full state vector, we need other mechanisms to determine what constraints to activate and how the input should be adjusted to keep the corresponding output function at its limit. These mechanisms should only rely on the observed system outputs $y_{i,t}$.

Let us define the *constraint errors* which measure deviations from the inequality constraint boundaries in (2) as follows

$$e_{i,t} = \gamma_i(\bar{y}_i - y_{i,t}), \quad i = 1, 2, \dots, p \quad (6)$$

where γ_i 's are some positive constants. The i -th inequality constraint in (2) is satisfied at time t if and only if $e_{i,t} \geq 0$, and it is said to be active when $e_{i,t} = 0$. The active constraint, *i.e.* the one that the bang-ride controller aims to ride, is then

$$i^*(t) = \arg \min_i \{e_{i,t}\} \quad (7)$$

Equation (7) yields in a switching mechanism based on the constraint errors (6) which, in contrast to (5), are directly measurable. For notational convenience, we sometimes drop the argument t and write $i^* = i^*(t)$.

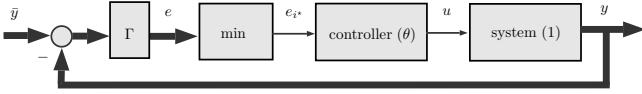


Fig. 1: The data-driven control scheme: The thick lines represent vector signals in \mathbb{R}^p and $\Gamma = \text{diag}(\gamma)$ is a non-negative diagonal matrix used to adjust the loop gains if necessary. The loop is only connected in one component at a time, which corresponds to the active constraint.

B. Active constraint riding

Once the constraint index i^* is determined, an appropriate control signal u_t is needed to bring the respective error in (6) to zero so that the selected constraint is ridden. This problem is equivalent to designing an output-feedback controller for the unknown plant (1) to track the reference signal $r_t = \bar{y}_i$.

For this purpose, we consider the control structure in Figure 1, where the controller block uses a fixed differentiable structure $u_t = C(\mathcal{H}_t, \theta_t)$ parametrized by $\theta_t \in \mathbb{R}^m$, where

$$\mathcal{H}_t = \{ (u_k, y_{i^*(k),k}) \mid 0 \leq k \leq t-1 \} \quad (8)$$

is the observed input-output data history just before t . Since an accurate model of the system dynamics is not available, we propose a learning-based control law whose parameters θ are adapted based on the observed data. The underlying algorithm that tunes the parameters attempts to minimize the one-step-ahead constraint error squared (6) at every time step, by solving the following online optimization problem

$$\begin{aligned} & \underset{\theta \in \Theta}{\text{minimize}} && J_t(\theta) = e_{i^*,t}^2 \\ & \text{subject to} && u_t = C(\mathcal{H}_t, \theta) \\ & && u, e_i \text{ satisfy (1), (6)} \end{aligned} \quad (9)$$

where $\Theta \subseteq \mathbb{R}^m$. The gradient of $J_t(\theta)$ at $\theta = \theta_t$ is given by

$$\nabla_{\theta} J_t(\theta_t) = -c_t e_{i^*,t} \nabla_{\theta} C(\mathcal{H}_t, \theta_t) \quad (10)$$

where

$$c_t = 2\gamma_{i^*} \frac{\partial h_{i^*}}{\partial u}(x_t, u_t) \quad (11)$$

Since the output functions are monotonic by Assumption 1 and $\gamma_i > 0$, c_t is non-negative. Thus, the vector

$$g_t = -e_{i^*,t} \nabla_{\theta} C(\mathcal{H}_t, \theta_t) \quad (12)$$

points to the exact gradient direction and is computable solely based on the observed data. Therefore, we use (12) to perform one projected gradient descent step, *i.e.*,

$$\theta_{t+1} = \text{proj}_{\Theta} \{ \theta_t - \alpha_t g_t \} \quad (13)$$

towards the optimal parameter $\theta = \theta_t^*$ that solves (9). The proposed method is summarized in Algorithm 1.

C. Convergence analysis

The theoretical performance of the proposed online algorithm are evaluated via their total regret

$$\mathcal{R}_{t_f} = \sum_{t=0}^{t_f} J_t(\theta_t) - J_t(\theta_t^*). \quad (14)$$

Algorithm 1 Data-driven bang-ride control:

Require: t_f, \bar{y}_i ($i = 1, 2, \dots, p$) ▷ input data.
Require: $\theta_0 \in \mathbb{R}^m$ ▷ initial parameters.

- 1: $t = 0, \mathcal{H}_0 = \emptyset, i^* = 1$
- 2: **while** $t \leq t_f$ **do**
- 3: $u_t \leftarrow C(\mathcal{H}_t, \theta_t)$.
- 4: Apply u_t and observe $y_{i,t}$ ($i = 1, 2, \dots, p$).
- 5: Compute i^* from (7). ▷ next constraint to ride.
- 6: Compute g_t from (12).
- 7: Update θ_{t+1} from (13).
- 8: $\mathcal{H}_{t+1} \leftarrow \mathcal{H}_t \cup \{(u_t, y_{i^*,t})\}$.
- 9: $t \leftarrow t + 1$
- 10: **end while**

In addition to the usual assumptions of convexity and boundedness, we assume that the sequence of optimizers in (9) is convergent. This assumption, which is also in place in the SPSA algorithm [19], is required for regret analysis. Because, unlike the usual setting for online convex optimization algorithms, the regret defined in (14) is not restricted to statically optimal solutions (constant sequences) [24].

Theorem 1: Assume $\Theta \subseteq \mathbb{R}^m$ is a bounded set, $\theta_0 \in \Theta$, $J_t(\theta)$ is convex in θ , $\varepsilon_t = \|\theta_{t+1}^* - \theta_t^*\| = O(t^{-\mu_2})$, and that Assumption 1 holds. Let the step size be

$$\alpha_t = \begin{cases} 1, & t = 0 \\ t^{-\mu_1}, & t > 0 \end{cases} \quad (15)$$

where $\mu_1 \in (0, 1)$ and $\mu_1 < \mu_2$. Let $\|g_t\|, |c_t| \leq G$ for some $G > 0$ and assume that the sequence $c_{t+1}/\alpha_{t+1} - c_t/\alpha_t$ changes sign a finite (possibly zero) number of times. Then the regret of Algorithm 1 satisfies

$$\mathcal{R}_{t_f} = O(t_f^{\mu^*}) \quad (16)$$

where $\mu^* = \max\{\mu_1, 1 - \mu_1, 1 + \mu_1 - \mu_2\}$.

Proof: Since the objective function $J_t(\theta)$ is convex,

$$J_t(\theta_t) - J_t(\theta_t^*) \leq \langle \nabla_{\theta} J_t(\theta_t), \theta_t - \theta_t^* \rangle \quad (17)$$

Since the projection operator is non-expansive, by using the relation (13) we obtain

$$\begin{aligned} \|\theta_{t+1} - \theta_t^*\|^2 &= \|\text{proj}_{\Theta} \{ \theta_t - \alpha_t g_t \} - \theta_t^*\|^2 \\ &\leq \|\theta_t - \alpha_t g_t - \theta_t^*\|^2 \\ &= \|\theta_t - \theta_t^*\|^2 + \alpha_t^2 \|g_t\|^2 - 2\alpha_t \langle g_t, \theta_t - \theta_t^* \rangle \end{aligned} \quad (18)$$

If $c_t = 0$ then $\nabla_{\theta} J_t(\theta_t) = c_t g_t = 0$ and thereby,

$$J_t(\theta_t^*) = J_t(\theta_t)$$

holds from (17), that is the corresponding regret term in (14) equals zero. By Assumption 1 and the fact that the scalars γ_i are positive, $c_t > 0$ holds from (11). Therefore to examine the worst-case regret, we assume $c_t \geq \epsilon > 0$. This allows writing (18) in terms of the gradient $g_t = \nabla_{\theta} J_t(\theta_t)/c_t$,

$$\begin{aligned} \langle \nabla_{\theta} J_t(\theta_t), \theta_t - \theta_t^* \rangle &\leq \\ \frac{c_t}{2\alpha_t} (\|\theta_t - \theta_t^*\|^2 - \|\theta_{t+1} - \theta_t^*\|^2) &+ \frac{\alpha_t}{2c_t} \|\nabla_{\theta} J_t(\theta_t)\|^2 \end{aligned} \quad (19)$$

By combining inequalities (17) and (19), we obtain

$$J_t(\theta_t) - J_t(\theta_t^*) \leq \frac{c_t}{2\alpha_t} (\|\theta_t - \theta_t^*\|^2 - \|\theta_{t+1} - \theta_t^*\|^2) + \frac{\alpha_t}{2c_t} \|\nabla_{\theta} J_t(\theta_t)\|^2 \quad (20)$$

Since

$$\|\theta_{t+1} - \theta_{t+1}^*\|^2 \leq \|\theta_{t+1} - \theta_t^*\|^2 + \|\theta_{t+1}^* - \theta_t^*\|^2 + 2\|\theta_{t+1}^* - \theta_t^*\| \|\theta_{t+1} - \theta_t^*\|$$

one has

$$-\|\theta_{t+1} - \theta_t^*\|^2 \leq \|\theta_{t+1}^* - \theta_t^*\|^2 + 2\|\theta_{t+1}^* - \theta_t^*\| \|\theta_{t+1} - \theta_t^*\| - \|\theta_{t+1} - \theta_{t+1}^*\|^2$$

which, when applied to (20), yields

$$J_t(\theta_t) - J_t(\theta_t^*) \leq \frac{\alpha_t}{2c_t} \|\nabla_{\theta} J_t(\theta_t)\|^2 + \frac{c_t}{2\alpha_t} (\|\theta_t - \theta_t^*\|^2 - \|\theta_{t+1} - \theta_{t+1}^*\|^2) + \frac{c_t}{2\alpha_t} (\|\theta_{t+1}^* - \theta_t^*\|^2 + 2\|\theta_{t+1}^* - \theta_t^*\| \|\theta_{t+1} - \theta_t^*\|) \quad (21)$$

where we have used $c_t > 0$. Summing both sides of (21) for $t = 0, 1, \dots, t_f$ and using the upper bound $\|\nabla_{\theta} J_t(\theta_t)\| = c_t \|g_t\| \leq G^2$ therein results

$$\sum_{t=0}^{t_f} J_t(\theta_t) - \sum_{t=0}^{t_f} J_t(\theta_t^*) \leq G^4 \sum_{t=0}^{t_f} \frac{\alpha_t}{2c_t} + \frac{c_0}{2\alpha_0} \|\theta_0 - \theta_0^*\|^2 + \sum_{t=0}^{t_f} \left(\frac{c_{t+1}}{2\alpha_{t+1}} - \frac{c_t}{2\alpha_t} \right) \|\theta_{t+1} - \theta_{t+1}^*\|^2 + \sum_{t=0}^{t_f} \frac{c_t}{2\alpha_t} \|\theta_{t+1}^* - \theta_t^*\| (\|\theta_{t+1}^* - \theta_t^*\| + 2\|\theta_{t+1} - \theta_t^*\|). \quad (22)$$

Since

$$\|\theta_t - \theta_t^*\|, \|\theta_{t+1}^* - \theta_t^*\|, \|\theta_{t+1} - \theta_t^*\| \leq \|\Theta\|$$

where $\|\Theta\| < \infty$ is the diameter of the bounded set Θ , it holds from (22) that

$$\begin{aligned} \sum_{t=0}^{t_f} J_t(\theta_t) - \sum_{t=0}^{t_f} J_t(\theta_t^*) &\leq G^4 \sum_{t=0}^{t_f} \frac{\alpha_t}{2c_t} + \|\Theta\|^2 \frac{c_0}{2\alpha_0} + \|\Theta\|^2 \sum_{t \in \mathcal{T}} \left(\frac{c_{t+1}}{2\alpha_{t+1}} - \frac{c_t}{2\alpha_t} \right) + \\ &3\|\Theta\| \sum_{t=0}^{t_f} \frac{c_t}{2\alpha_t} \|\theta_{t+1}^* - \theta_t^*\| \\ &\leq \frac{G^4}{2} \sum_{t=0}^{t_f} \frac{\alpha_t}{c_t} + \|\Theta\|^2 \frac{c_0}{2\alpha_0} + \frac{\|\Theta\|^2}{2} \sum_{t \in \mathcal{S}} \frac{c_{t+1}}{\alpha_{t+1}} \\ &+ \frac{3\|\Theta\|}{2} \sum_{t=0}^{t_f} \frac{c_t}{\alpha_t} \varepsilon_t \end{aligned} \quad (23)$$

where $\mathcal{T} = \{t \in [0, t_f] | c_{t+1}/\alpha_{t+1} > c_t/\alpha_t\}$ and \mathcal{S} is a finite subset of \mathcal{T} . With a large enough t_f , there exist some $\tau \geq 0$

and $M_0 > 0$ such that $\varepsilon_t \leq M_0 t^{-\mu_2}$ holds for $\tau < t \leq t_f$. Therefore, by using the step size (15) in (23) we obtain

$$\begin{aligned} \sum_{t=0}^{t_f} J_t(\theta_t) - \sum_{t=0}^{t_f} J_t(\theta_t^*) &\leq \frac{G^4}{2\epsilon} \left(1 + \sum_{t=1}^{t_f} t^{-\mu_1} \right) \\ &+ \|\Theta\|^2 \frac{G}{2} (1 + |\mathcal{S}|(t_f + 1)^{\mu_1}) \\ &+ \|\Theta\|^2 \frac{3G}{2} \left(\sum_{t=0}^{\tau} \frac{\varepsilon_t}{\alpha_t} + M_0 \sum_{t=\tau+1}^{t_f} t^{\mu_1 - \mu_2} \right) \end{aligned}$$

where $|\mathcal{S}| < \infty$ is the cardinality of the set \mathcal{S} . Therefore when $\mu_2 \neq 1 + \mu_1$, the regret of Algorithm 1 satisfies

$$\begin{aligned} \mathcal{R}_{t_f} &\leq \frac{G^4}{2\epsilon} \left(2 + \int_1^{t_f} t^{-\mu_1} dt \right) + \|\Theta\|^2 \frac{G}{2} (1 + |\mathcal{S}|(t_f + 1)^{\mu_1}) \\ &+ \|\Theta\|^2 \frac{3G}{2} \left(\sum_{t=0}^{\tau} \frac{\varepsilon_t}{\alpha_t} + M_0(\tau + 1)^{\mu_1 - \mu_2} \right) \\ &+ M_0 \|\Theta\|^2 \frac{3G}{2} \int_{\tau+1}^{t_f} t^{\mu_1 - \mu_2} dt \\ &\leq M_1 + M_2 t_f^{1 - \mu_1} + M_3 t_f^{\mu_1} + M_4 t_f^{1 + \mu_1 - \mu_2} \end{aligned} \quad (24)$$

for some positive constants M_1, M_2, M_3 and M_4 . When $\mu_2 = 1 + \mu_1$, on the other hand, a similar calculation yields

$$\mathcal{R}_{t_f} \leq M_1 + M_2 t_f^{1 - \mu_1} + M_3 t_f^{\mu_1} + M_4 \log(t_f) \quad (25)$$

In either case, both inequalities (24) and (25) imply

$$\mathcal{R}_{t_f} \leq M t_f^{\mu^*}$$

for a large enough $t_f > 0$ and some $M > 0$. \blacksquare

Theorem 1 asserts that the regret of Algorithm 1 is sublinear when $\mu^* < 1$. The minimum order of regret provable by Theorem 1 is

$$\begin{aligned} \mu^* &= \min_{\mu_1} \max\{1 - \mu_1, \mu_1, 1 + \mu_1 - \mu_2\} \\ &= \begin{cases} 1 - \mu_2/2 & \text{if } \mu_2 \in (0, 1) \\ 1/2 & \text{if } \mu_2 \geq 1 \end{cases} \end{aligned}$$

attained for $\mu_1 = \min\{1/2, \mu_2/2\}$. If $\mu_2 \geq 1$, this agrees with the order of regret $\mu^* = 1/2$ in [24]. When the summand in (14) has a limit, a sublinear regret implies convergence to an optimal solution, that is,

$$\lim_{t \rightarrow +\infty} J_t(\theta_t) - J_t(\theta_t^*) = 0. \quad (26)$$

IV. NUMERICAL EXPERIMENTS

In this section, we evaluate our model-free charging method on a few common battery fast-charging problems.

A. SPMET cell

We first consider the nonlinear (discretized) single-particle battery model augmented by electrolyte and temperature states (SPMeT). The input is the applied current u , the output is the terminal voltage V and state of charge (SOC) and the state vector x is

$$x = [c^{a,-} \quad c^{s,-} \quad c^{e,-} \quad c^{e,+} \quad T] \quad (27)$$

where $c^{a,-}$ and $c^{s,-}$ are the average and surface concentration of lithium in the negative particle, respectively, $c^{e,\pm}$ is the electrolyte lithium-ion concentration and T the temperature. It is assumed that the diffusion in the positive particle is infinitely fast such that its concentration is obtained from the mass balance. The particle average and surface concentration are described by an equivalent hydraulic model as in [16]. Diffusion of lithium-ions in the electrolyte is modeled by a Padé approximated transfer function as in [23]. The resulting model is

$$\begin{aligned}
c_{t+1}^{a,-} &= c_t^{a,-} + \frac{\Delta t}{V_p^- F} u_t \\
c_{t+1}^{s,-} &= \frac{\mathcal{G} \Delta t}{\beta(1-\beta)\tau^-} c_t^{a,-} + \left(1 - \frac{\mathcal{G} \Delta t}{\beta(1-\beta)\tau^-}\right) c_t^{s,-} \\
&\quad + \frac{\Delta t}{V_p^- F(1-\beta)} u_t \\
c_{t+1}^{e,-} &= c_t^{e,-} + \frac{\Delta t D^- N_1^-}{L^- \varepsilon^- N_3^-} (c_0^{e,-} - c_t^{e,-}) + \frac{\Delta t N_2^-}{V_e^- F N_3^-} u_t \\
c_{t+1}^{e,+} &= c_t^{e,+} + \frac{\Delta t D^+ N_1^+}{L^+ \varepsilon^+ N_3^+} (c_0^{e,+} - c_t^{e,+}) + \frac{\Delta t N_2^+}{V_e^+ F N_3^+} u_t \\
T_{t+1} &= T_t - a \Delta t (T_t - T_a) \\
&\quad + b \Delta t (\Delta \eta(u_t, x_t) + \Delta \Phi_e(u_t, x_t)) u_t \\
V_t &= \Delta U(x_t) + \Delta \eta(u_t, x_t) + \Delta \Phi_e(u_t, x_t) \\
SOC_t &= \frac{c_t^{a,-} / c_{\max}^- - \theta_1}{\theta_2 - \theta_1}
\end{aligned} \tag{28}$$

where Δt is the discrete time step, V_p aggregated particle volume, F Faraday constant, τ solid diffusion time constant, L electrode thickness, ε porosity, D^\pm diffusion coefficient, V_e electrolyte volume, c_{\max}^- maximum concentration and θ stoichiometric points defining SOC. Refer to [16, 23] for computation of constants \mathcal{G} , β , N_1^\pm , N_2^\pm , N_3^\pm . Lastly, ΔU , $\Delta \eta$ and $\Delta \Phi_e$ are non-linear functions that describe differences in open circuit potentials, overpotentials, and electrolyte potentials between the positive and negative electrodes. We consider a charging horizon of $t_f = 3000$ with the initial conditions

$$\begin{aligned}
c_0^{a,-} &= c_0^{s,-} = 0.1 c_{\max}^-, \\
T_0 &= 25, \\
c_0^{e,-} &= c_0^{e,+} = 1200,
\end{aligned}$$

while enforcing the following bounds on the charging current and the terminal voltage

$$\begin{aligned}
u_t &\leq 2Q = 56.3739, \\
V_t &\leq 4.2
\end{aligned} \tag{29}$$

where Q is the capacity. The objective is to maximize SOC which is equivalent to

$$\sum_{t=0}^{t_f} c_t^{a,-},$$

as $c^{a,-}$ has a monotone relation with SOC according to (28). One may implement the ideal bang-ride protocol (5), by

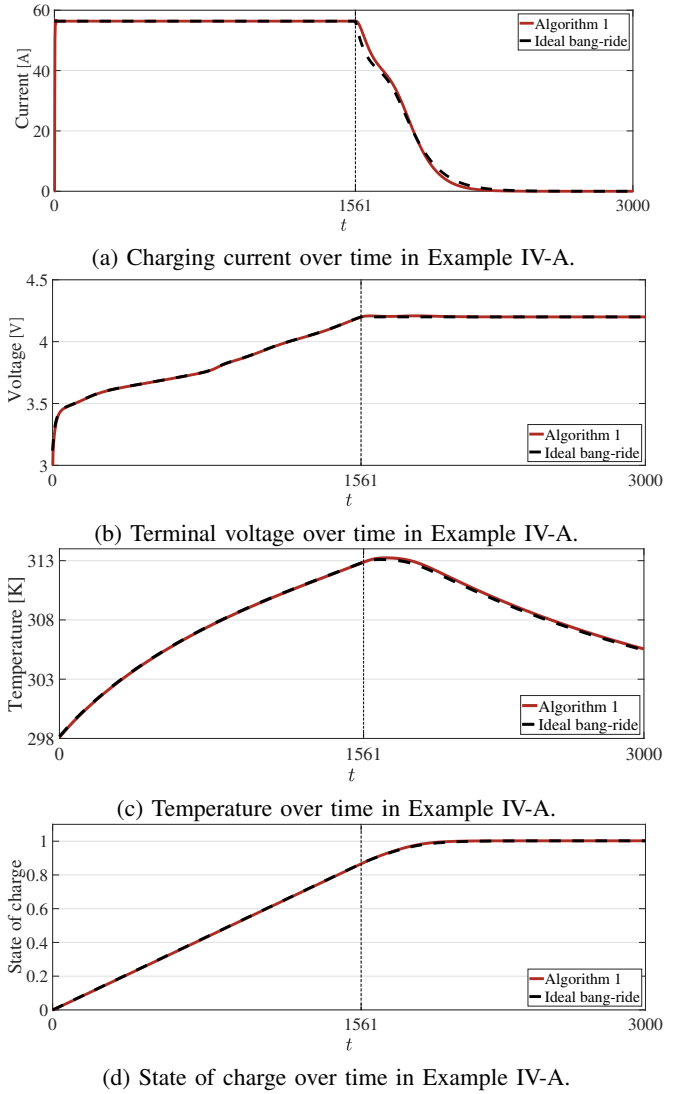


Fig. 2: The battery is charged with the maximum current until the terminal voltage constraint in (29) is activated at $t = 1561$, after which, the battery is charged with a constant voltage in Example IV-A.

solving the constraint equations (4) analytically using the model (28). However, this is not possible, when the battery model is not available. In this case, one can use Algorithm 1 to obtain the bang-ride charging current, by assuming a simple PI controller structure as follows

$$u_t = C(\mathcal{H}_t, \theta_t) = [\theta_t]_1 e_{i^*(t-1), t-1} + [\theta_t]_2 \sum_{k=0}^{t-1} e_{i^*(k), k} \tag{30}$$

where $[\theta_t]_1 = K_p$ and $[\theta_t]_2 = K_i$ are the PI gains. The error weights γ_i in (6) are equally chosen, *i.e.* $\Gamma = \text{diag}(\gamma) = I$. In Figure 2, the resulting charging current, terminal voltage, temperature, and the state-of-charge are compared with those obtained from an ideal bang-ride solution derived from the battery model analytically. The resulting charging profile is of CCCV form, as can be seen in Figure 2.

B. ECM cell

In the next example, we consider a continuous-time equivalent circuit battery model (ECM) with two time constants, augmented with the lumped thermal model [7]. This simple model is used to evaluate our algorithm against the bang-ride charging protocols computed from a large number of randomly generated perturbed models. We use the notation u for the charging current, T for the temperature, SOC for the state of charge, and v_1, v_2 for the voltages across the (abstract) RC-links. This model is described by the following ordinary differential equations:

$$\begin{aligned} \dot{v}_1(t) &= -\frac{1}{R_1 C_1} v_1(t) + \frac{1}{C_1} u(t) \\ \dot{v}_2(t) &= -\frac{1}{R_2 C_2} v_2(t) + \frac{1}{C_2} u(t) \\ \dot{SOC}(t) &= \frac{1}{Q} u(t) \\ \dot{T}(t) &= -a(T(t) - T_a) + bu(t)v_d(t), \end{aligned} \quad (31)$$

where $v_d(t) = R_o u(t) + v_1(t) + v_2(t)$ is called the dynamic voltage. The battery model (31) can be written as a nonlinear monotone dynamic system of the form (1) after discretization with an appropriate sampling time Δt . In this model, the measurable signals are the input current, terminal voltage, and the cell temperature, based on which we define the following outputs

$$\begin{aligned} h_1(x_t, u_t) &= u_t, \\ h_2(x_t, u_t) &= K x_t + u_t, \\ h_3(x_t, u_t) &= T_{t+1} - T_a \\ &= [x_t]_4 (1 - a\Delta t) + b\Delta t C x_t u_t + b\Delta t R_o u_t^2 \end{aligned}$$

where $C, K \in \mathbb{R}^{1 \times 4}$ are constant, $[x_t]_3$ is the state of charge, and $[x_t]_4 = T_t - T_a$ is the temperature variation of the cell with respect to ambient at time t . Now consider the fast charging problem (2) with $L(x_t, u_t) = [x_t]_3$. In addition to current and voltage constraints, we impose a constraint on the cell temperature. This additional constraint is known to help with limiting degradation and sustaining the negative electrode performance [13]. These constraints can be written as $y_{i,t} \leq \bar{y}_i$ where

$$\begin{aligned} \bar{y}_1 &= u_{\max}, \\ \bar{y}_2 &= v_{\max}, \\ \bar{y}_3 &= T_{\max} - T_a \end{aligned}$$

We consider a simple PI controller as (30) in Algorithm 1. The charging current, dynamic voltage, and the cell temperature following the model-free charging algorithm provided in this paper are plotted in Figure 3 (solid red and blue), along with those of the ideal bang-ride charging protocol (dashed black). The charging current from Algorithm 1 is computed online based on the input-output data, whereas the bang-ride charging currents are obtained analytically, by solving the constraint equations (4) and selecting the minimum state-feedback control signals (5). We also computed the ideal bang-ride currents for 1000 different random

ECMs whose parameters differed from the true values by a maximum of 10%. The resulting currents, dynamic voltages, and temperatures of the true battery under these protocols are plotted in solid gray. The bang-ride protocols computed from these perturbed models can violate the constraints or lead to sub-optimal operation. In contrast, Algorithm 1 tracks the ideal bang-ride protocol without having access to the (even inaccurate) model of the battery (see Figure 3).

As can be seen in Figure 3, when the error signals (6) are not scaled properly ($\Gamma = I$) the model-free approach is slow in tracking the ideal bang-ride charging protocol once the temperature constraint is switched on. The reason is that the temperature dynamics are substantially slower than the voltage or the current dynamics and when it is switched on, the controller gains θ struggle to adapt to the abrupt change. As can be seen in Figure 1, this problem is easily treated by scaling the measured errors so that they are roughly in the same order of magnitude as follows

$$\Gamma = \begin{bmatrix} 1 & 0 & 0 \\ 0 & 1 & 0 \\ 0 & 0 & 500 \end{bmatrix} \quad (32)$$

C. ECM pack

As the final experiment, we consider a pack of 100 battery cells each described by an augmented ECM (31), but with modified temperature dynamics to account for the heat exchanged between adjacent cells in the pack as follows [15]

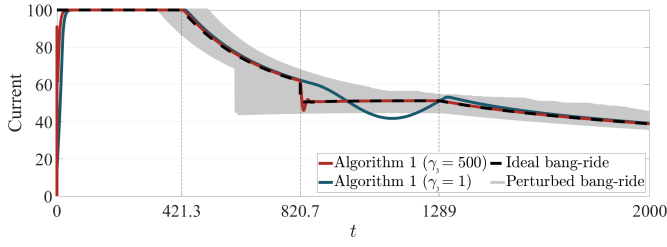
$$\begin{aligned} \dot{T}_i(t) &= -a(T_i(t) - T_a) \\ &+ bu(t)(R_o u(t) + v_{i,1}(t) + v_{i,2}(t)) \\ &+ k_1(T_{i-1}(t) - T_i(t)) + k_2(T_{i+1}(t) - T_i(t)) \end{aligned} \quad (33)$$

where k_1 and k_2 are some positive constants and T_i is the temperature of the i -th cell. For convenience, when $i = 1$ and $i = 100$, we take $T_0(t) = T_{100}(t)$ and $T_{101}(t) = T_1(t)$ in (33) respectively. The parameters of the RC links in the equivalent circuit models are slightly varied between the cells. The cells are assumed to be connected in series, so by Kirchhoff laws, the same input current $u(t)$ goes through all of them and the overall pack terminal voltage equals the sum of the terminal voltages of all cells as follows

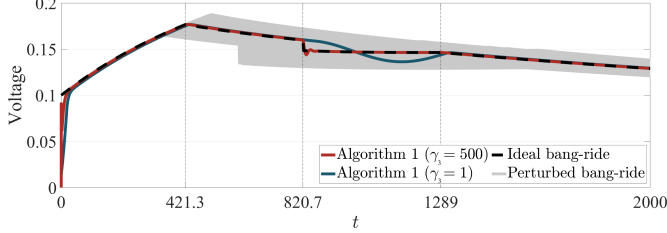
$$V(t) = V_1(t) + V_2(t) + \dots + V_{100}(t)$$

where $V_i(t) = v_{i,1}(t) + v_{i,2}(t) + R_o u(t) + v_{ocv}$ is the terminal voltage of the i -th cell and v_{ocv} is the cell open-circuit voltage. This model can be discretized with an appropriate sampling time Δt to obtain the battery pack model (1), with the measurable outputs defined as follows

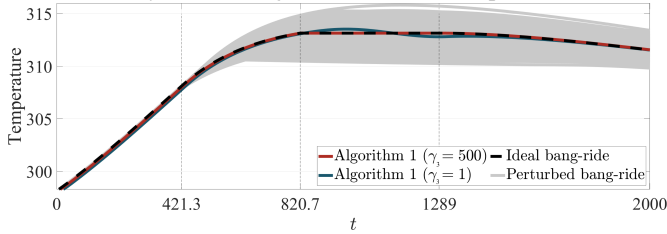
$$\begin{aligned} h_i(x_t, u_t) &= u_t, & i = 1 \\ h_i(x_t, u_t) &= K x_{i,t} + u_t, & 2 \leq i \leq 101 \\ h_i(x_t, u_t) &= [x_{i,t}]_4 (1 - a\Delta t) \\ &+ b\Delta t C x_{i,t} u_t + b\Delta t R_o u_t^2 \\ &+ \Delta t k_1 ([x_{i-1,t}]_4 - [x_{i,t}]_4) \\ &+ \Delta t k_2 ([x_{i+1,t}]_4 - [x_{i,t}]_4), & 102 \leq i \leq 201 \\ h_i(x_t, u_t) &= h_j(x_t, u_t) - h_k(x_t, u_t), & 202 \leq i \leq 10201 \end{aligned}$$



(a) Charging current over time in Example IV-B.



(b) Dynamic voltage over time in Example IV-B.



(c) Temperature over time in Example IV-B.

Fig. 3: The active constraint changes three times in Example IV-B. In the beginning, the current constraint ($y_{1,t} = u_{\max}$) is active to charge with the maximum current until $t = 421.3$, when the current constraint is switched to the voltage constraint. The voltage constraint is active until $t = 820.7$ before the active constraint is switched to the temperature constraint. Finally, the active constraint is switched back to the voltage constraint at $t = 1289$ which remains active until the end of the experiment.

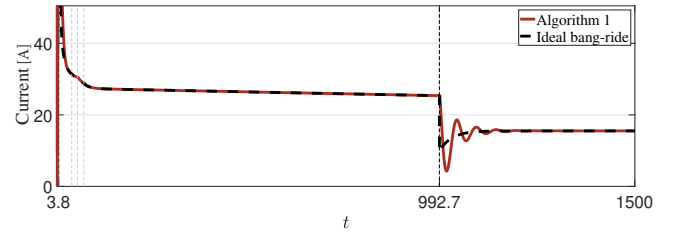
where the last 10000 output functions are constructed by the differences between the temperature variations of any two cells within the pack, *i.e.*, $j, k \in \{102, 103, \dots, 201\}$. We consider the fast charging problem (2) with the total state of charge

$$L(x_t, u_t) = \sum_{i=1}^{100} [x_{i,t}]_3.$$

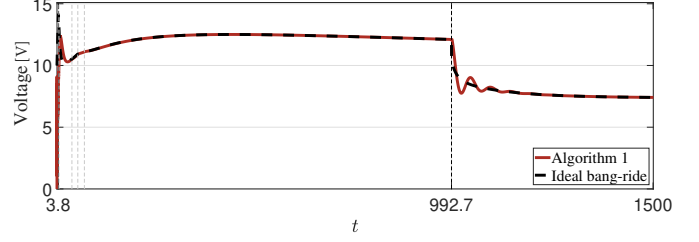
In addition to the constraints on every cell voltage and temperature, we also impose a constraint on the differences between the cells' temperatures. The purpose of this constraint is to achieve a uniform degradation of the cells. All the constraints can be written in the form $y_{i,t} \leq \bar{y}_i$, where

$$\begin{aligned} \bar{y}_i &= u_{\max}, & i &= 1 \\ \bar{y}_i &= v_{\max}, & i &= 2, 3, \dots, 101 \\ \bar{y}_i &= T_{\max} - T_a, & i &= 102, 103, \dots, 201 \\ \bar{y}_i &= \Delta T_{\max}, & i &= 202, 203, \dots, 10201 \end{aligned}$$

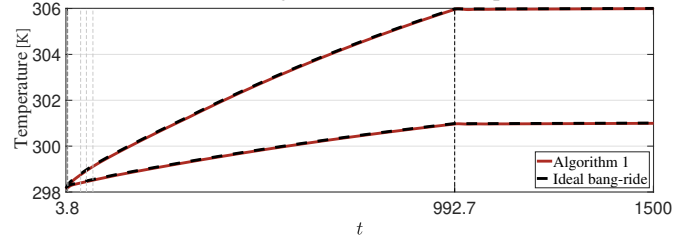
and $\Delta T_{\max} = 5$ is the maximum allowable temperature difference between any two cells in the pack. The error



(a) Charging current over time in Example IV-C.



(b) Terminal voltage over time in Example IV-C.



(c) Temperature over time in Example IV-C.

Fig. 4: Under the ideal bang-ride charging approach in Example IV-C, the battery is charged with the maximum current $u_t = u_{\max}$ until $t = 3.8$ when a cell voltage constraint is activated. After that, the active voltage constraint is exchanged several times among different cells in the pack until $t = 992.7$ when it is handed over to a temperature difference constraint. The last activated constraint maintains a difference of ΔT_{\max} between the cells' temperatures in the pack.

weights in (6) are chosen as

$$\begin{aligned} \gamma_i &= 1, & i &= 1, 3, \dots, 101 \\ \gamma_i &= 500, & i &= 102, 103, \dots, 10201. \end{aligned}$$

Similar to Examples IV-A and IV-B, we consider a simple PI controller structure as (30) in Algorithm 1. The resulting charging current, the overall pack voltage, and the maximum and minimum temperatures among the cells in the pack are shown in Figure 4.

V. CONCLUSION

We considered a general battery fast charging problem with various constraints in this paper. We proposed a model-free algorithm that converges to the ideal bang-ride protocol, by observing the charging data without accessing the battery model or its states. The numerical examples demonstrate that the proposed model-free approach can be more effective than first identifying an (imperfect) model for the battery and then computing its optimal charging profile.

In future work, it would be interesting to investigate if it is possible to ensure that the proposed algorithm stays in the feasible region at all times, satisfying the desired charging constraints. Since any overshoot in the data-driven closed-loop system (Figure (1)) as $e_{i^*,t} < 0$ results in a violation of the active constraint, developing data-driven output-feedback controllers that can track a reference with no overshoots would provide constraint satisfaction guarantees for our data-driven algorithm. However, this can potentially lead to overly cautious charging strategies, which would result in large regrets. This is the case when the closed-loop system in Figure (1) has a slow response. Therefore, the model-free charging method proposed in this paper can benefit from developing a data-driven controller design that can achieve a non-overshooting closed-loop response with a fast decay rate for a system with unknown dynamics.

REFERENCES

- [1] Malin Andersson et al. “Informative battery charging: integrating fast charging and optimal experiments”. In: *IFAC-PapersOnLine* 56.2 (2023), pp. 11160–11166.
- [2] Ross Drummond et al. “Constrained optimal control of monotone systems with applications to battery fast-charging”. In: *arXiv preprint arXiv:2301.07461* (2023).
- [3] Yuhan Hao et al. “Adaptive Model-Based Reinforcement Learning for Fast Charging Optimization of Lithium-Ion Batteries”. In: *IEEE Transactions on Industrial Informatics* (2023).
- [4] Elad Hazan et al. “Introduction to online convex optimization”. In: *Foundations and Trends® in Optimization* 2.3-4 (2016), pp. 157–325.
- [5] Håkan Hjalmarsson, Svante Gunnarsson, and Michel Gevers. “A convergent iterative restricted complexity control design scheme”. In: *Proceedings of 1994 33rd IEEE conference on decision and control*. Vol. 2. IEEE, 1994, pp. 1735–1740.
- [6] Zhong-Sheng Hou and Zhuo Wang. “From model-based control to data-driven control: Survey, classification and perspective”. In: *Information Sciences* 235 (2013), pp. 3–35.
- [7] Xiaosong Hu et al. “A comparative study of control-oriented thermal models for cylindrical Li-ion batteries”. In: *IEEE Transactions on Transportation Electrification* 5.4 (2019), pp. 1237–1253.
- [8] Benben Jiang and Xizhe Wang. “Constrained bayesian optimization for minimum-time charging of lithium-ion batteries”. In: *IEEE Control Systems Letters* 6 (2021), pp. 1682–1687.
- [9] Weihang Li et al. “Data-driven systematic parameter identification of an electrochemical model for lithium-ion batteries with artificial intelligence”. In: *Energy Storage Materials* 44 (2022), pp. 557–570.
- [10] Yang Li et al. “Electrochemical model-based fast charging: Physical constraint-triggered PI control”. In: *IEEE Transactions on Energy Conversion* 36.4 (2021), pp. 3208–3220.
- [11] Praveen Nambisan, Pankaj Saha, and Munmun Khanra. “Real-time optimal fast charging of Li-ion batteries with varying temperature and charging behaviour constraints”. In: *Journal of Energy Storage* 41 (2021), p. 102918.
- [12] Marko Nonhoff and Matthias A Müller. “Online convex optimization for data-driven control of dynamical systems”. In: *IEEE Open Journal of Control Systems* 1 (2022), pp. 180–193.
- [13] M Rosa Palacin. “Understanding ageing in Li-ion batteries: a chemical issue”. In: *Chemical Society Reviews* 47.13 (2018), pp. 4924–4933.
- [14] Saehong Park et al. “Optimal control of battery fast charging based-on Pontryagin’s minimum principle”. In: *2020 59th IEEE Conference on Decision and Control (CDC)*. IEEE, 2020, pp. 3506–3513.
- [15] Andrea Pozzi and Davide M Raimondo. “Stochastic model predictive control for optimal charging of electric vehicles battery packs”. In: *Journal of Energy Storage* 55 (2022), p. 105332.
- [16] Raffaele Romagnoli et al. “A feedback charge strategy for Li-ion battery cells based on reference governor”. In: *Journal of process control* 83 (2019), pp. 164–176.
- [17] Richard Schmich et al. “Performance and cost of materials for lithium-based rechargeable automotive batteries”. In: *Nature Energy* 3.4 (2018), pp. 267–278.
- [18] Andrea Simonetto et al. “Time-varying convex optimization: Time-structured algorithms and applications”. In: *Proceedings of the IEEE* 108.11 (2020), pp. 2032–2048.
- [19] James C Spall. “Multivariate stochastic approximation using a simultaneous perturbation gradient approximation”. In: *IEEE transactions on automatic control* 37.3 (1992), pp. 332–341.
- [20] Hamed Taghavian, Ross Drummond, and Mikael Johansson. “When are selector control strategies optimal for constrained monotone systems?” In: *arXiv preprint arXiv:2312.08829* (2023).
- [21] Anna Tomaszewska et al. “Lithium-ion battery fast charging: A review”. In: *ETransportation* 1 (2019), p. 100011.
- [22] Chaolun Wang, Tengfei Xiao, and Xiao-Dong Li. “Iterative learning control with optimal learning gain for recharging of Lithium-ion battery”. In: *2019 IEEE 8th Data Driven Control and Learning Systems Conference (DDCLS)*. IEEE, 2019, pp. 1117–1121.
- [23] Shifei Yuan et al. “A transfer function type of simplified electrochemical model with modified boundary conditions and Pade approximation for Li-ion battery: Part 2. Modeling and parameter estimation”. In: *Journal of Power Sources* 352 (2017), pp. 258–271.
- [24] Martin Zinkevich. “Online convex programming and generalized infinitesimal gradient ascent”. In: *Proceedings of the 20th international conference on machine learning (icml-03)*. 2003, pp. 928–936.